Am J Transl Res 2025;17(3):1679-1693
www.ajtr.org /ISSN:1943-8141/AJTR0161582

Original Article

circRNA_0005927 inhibits gastric cancer metastasis by downregulating the miR-570-3p/FOXO3 axis

Gao Zhou[1*], Jian Wen[2*], Feng Lu[1], Jianhua Wang[1], Shuguang Tan[1]

[1]*Department of Gastrointestinal Surgery, Hengyang Central Hospital, Hengyang 421001, Hu'nan, China;* [2]*Department of Anesthesiology, Hengyang Central Hospital, Hengyang 421001, Hu'nan, China.* [*]*Equal contributors.*

Received October 30, 2024; Accepted February 9, 2025; Epub March 15, 2025; Published March 30, 2025

Abstract: Objective: This study aimed to explore the effects of circ_0005927 on proliferation, invasion, and epithelial-mesenchymal transformation (EMT) in gastric cancer (GC) cells through its negative modulation of the miR-570-3p/FOXO3 axis. Methods: The expression levels of circ_0005927, miR-570-3p, and FOXO3 in GC tissues and cells were measured using quantitative reverse transcription polymerase chain reaction (qRT-PCR). Proliferation, colony formation, invasion, and EMT were assessed by MTT assay, colony formation assay, Transwell assay and western blotting, respectively. RNase R digestion and nuclear-cytoplasmic fractionation were performed to evaluate the properties of circ_0005927. A dual luciferase reporter assay was conducted to verify the interaction between circ_0005927, miR-570-3p, and FOXO3. Results: Circ_0005927 and FOXO3 expression were significantly lower in GC tissues compared to adjacent normal tissues, while miR-570-3p was upregulated (all $P<0.05$). Low circ_0005927 and high miR-570-3p expression were associated with poor prognosis in GC patients (both $P<0.05$). In GC cells, circ_0005927 mediated FOXO3 expression by binding to miR-570-3p ($P<0.05$). Overexpression of circ_0005927 inhibited GC cell proliferation, colony formation, invasion and EMT, whereas overexpression of miR-570-3p or FOXO3 knockdown partially reversed these effects (all $P<0.05$). Conclusion: Circ_0005927 inhibits the proliferation, colony formation, invasion and EMT of GC cells through the upregulation of FOXO3, facilitated by the sequestration of miR-570-3p. Targeting the circ_0005927/miR-570-3p/FOXO3 axis may offer a promising therapeutic approach for GC.

Keywords: Circ_0005927, miR-570-3p, FOXO3, gastric cancer, metastasis

Introduction

Gastric cancer (GC) is the fifth most common malignant tumor and the third most common cause of death worldwide [1]. The incidence and fatality rate of GC are increasing year by year, and there is an urgent need to improve the early diagnosis and treatment of GC to improve the prognosis of GC patients [2].

CircRNAs are a type of endogenous non-coding RNAs discovered in recent years, which have a unique closed circular structure and are generated by the reverse splicing of precursor mRNA [3]. With the development of RNA sequencing technology, thousands of circRNAs have been discovered. Previous studies have shown that circRNAs may be involved in the occurrence, development, and metastasis of GC. For example, circ_0049447 acts by inhibiting the proliferation, migration, invasion, and epithelial mesenchymal transformation (EMT) of GC cells [4]. Circ_0005927 originates from VDAC3 and it is mainly located on chr8:42259305-42260979 [5]. However, the mechanism of circ_0005927 in GC has not been reported yet. Therefore, in this study, the possible role and regulatory mechanism of circ_0005927 in GC were investigated.

MicroRNAs (miRNAs) are non-coding single-stranded RNA molecules with a length of 21 to 25nt. Currently, numerous studies have confirmed that circRNAs, as endogenous competing RNA, can play a role in GC progression through the competitive adsorption of miRNAs. For example, circHECTD1 promotes the malignant progression of GC through miR-137/PBX3 axis regulation [6]. In addition, although hsa-miR-570-3p has been found to play a pro-can-

https://doi.org/10.62347/VPOU7494

cer role in tumors [7], the function and mechanism of miR-570-3p in GC still need to be further clarified. FOXO3 is a human protein encoded by the FOXO3 gene, also known as Forkhead box O3 or FOXO3a. FOXO3 expression is significantly reduced in GC, and FOXO3 can inhibit GC cell proliferation and induce cell apoptosis [8]. Therefore, in this study, the role and mechanism of circ_0005927/miR-570-3p/FOXO3 axis in GC were explored.

In this study, it was postulated that by inhibiting miR-570-3p and up-regulating FOXO3, circ_0005927 inhibits the proliferation, colony formation, invasion and EMT of GC cells. circ_0005927/miR-570-3p/FOXO3 axis might provide a new basis for GC treatment.

Methods

Bioinformatic analysis

The gene expression dataset for GC-related circRNAs (GSE78092) was retrieved from the NCBI database (https://www.ncbi.nlm.nih.gov), which includes data from 3 GC samples and 3 adjacent normal tissues. Differentially expressed circRNAsin GC were identified using the limma package, with filtering criteria set at an adjusted *P*-value <0.05 and |LogFoldChange| >1. To predict the interaction between circ_0005927 and miR-570-3p, the RNA22 tool (https://cm.jefferson.edu/rna22/) was employed. The downstream target genes of miR-570-3p were predicted using multiple online prediction tools, including TargetScan (http://www.targetscan.org/vert_72/), miRDB (http://mirdb.org) and miRWalk (http://mirwalk.umm.uni-heidelberg.de). Gene Ontology (GO) enrichment analysis of the predicted target genes was conducted using the DAVID online tool (https://david.ncifcrf.gov). Risk-associated GC genes (c1708349) were obtained from the DisGeNET database (http://disgenet.org), with the screening threshold set at a GDA score >0.4 (including CDH1, IL1RN and KRAS). Protein-protein interaction (PPI) networks were constructed using the STRING database (http://string-db.org).

Collection of tissues

Ninety pairs of GC tissues and adjacent normal tissues (≥3 cm from the tumor margin) were collected from patients who received treatment in the Gastrointestinal, Hernia and Abdominal Surgery Department of Hengyang Central Hospital between April 2019 and March 2021. All specimens were rinsed with cold saline and immediately frozen in liquid nitrogen or stored at -80°C until further use. Inclusion criteria: (1) Patients with histopathologically confirmed GC; (2) Patients who had not received preoperative radiotherapy or chemotherapy. Exclusion criteria: (1) Patients with recurrent GC; (2) Patients with comorbid conditions. Prior to sample collection, all GC patients provided written informed consent. This study was approved by the Ethics Committee of Hengyang central Hospital.

Cell culture

Human GC cell lines (XGC-1, NCI-N87, MCG-7901 and MGC-803), the human normal gastric mucosal cell line GES-1, and 293T cells were purchased from the Cell Bank of the Committee for the Preservation of Typical Cultures, Chinese Academy of Sciences (Shanghai, China). Cells were cultured in Dulbecco's Modified Eagle Medium (DMEM) containing 10% fetal bovine serum (PM150210, Wuhan Nopsy Life Science Co., Ltd., China) and supplemented with 1% penicillin/streptomycin (C0222, Shanghai Biyuntian Biotechnology Co., Ltd., China). All cultures were maintained in a humidified incubator at 37°C with 5% CO_2.

Cell transfection

The circ_0005927 overexpression vector (oe-circ) and its corresponding negative control (oe-NC), miR-570-3p mimics and the negative control RNA (miR-NC), as well as small interfering RNA targeting FOXO3 (si-FOXO3) and its negative control (si-NC), were purchased from Guangzhou Ruibo Biological Technology Co., Ltd. Before transfection, XCG-1 cells were inoculated in 6-well plates at 30% fusion degree. The cells were then transfected using Lipofectamine 3000 reagent (L3000001, Thermo Fisher Scientific, USA). Transfection efficiency was assessed by quantitative reverse transcription polymerase chain reaction (qRT-PCR). The sequences used for transfection are listed in **Table 1**.

MTT assay

Cell proliferation was assessed using the MTT kit (C0009S, Shanghai Biyuntian Biotechnology

Table 1. Interference or overexpression sequences

Name	Sequences (5'-3')
oe-circ	CUACAAAGGGAAGCACUUUCUC
oe-NC	CCCTCGAGGGATGCTCGAATGACAT
miR-570-3p mimic	CUACAAAGGGAAGCACUUUCUC
miR-NC	CAACAAAUCACCGCCUGCCAUA
si-FOXO3	TTCTCCGAACGTGTCACGT
si-NC	CAGAUUUUAUGCAACUAAA

Co., Ltd., China). Transfected XCG-1 cells were collected to prepare cell suspension, and the cells were inoculated in 96-well plates at a density of 3×10^3 cells per well. After incubation for 24, 48 and 72 h, 20 μL of MTT solution was added to each well and incubated for an additional 4 h. Subsequently, 100 mL of dimethyl sulfoxide (DMSO) was added to each well, and the plate was shaken at low speed for 10 min. The absorbance was measured at 490 nm using a microplate reader (ML-DR3518, Shanghai Enzyme Link Biotechnology Co., Ltd., China).

Colony formation assay

Transfected XGC-1 cells (5×10^3 cells/well) were seeded in 6-well plates with RPMI-1640 medium (PM150110B, Wuhan Nopse Life Science and Technology Co., Ltd., China) to assess colony formation. After 10 days of culture, colonies were fixed with 4% paraformaldehyde (P1110, Beijing Solibul Technology Co., Ltd., China) and stained with 0.1% crystal violet (C8470, Beijing Solibul Technology Co., Ltd., China). Colonies were then counted using an inverted microscope (WMF-3690, Shanghai Wumo Optical Instrument Co., Ltd., China).

Transwell assay

The invasive ability of XGC-1 cells was evaluated using Transwell chambers (8 μm pore size, Corning, New York, USA). Transfected XGC-1 cells were trypsinized (T1300, Beijing Solebo Technology Co., Ltd., China), washed with PBS, and resuspended to prepare a cell suspension. A total of 300 μL of the cell suspension was added into the upper chamber, which was precoated with Matrigel matrix gel, while 700 μL of RPMI-1640 medium was added to the lower chamber. After 24 hours of incubation at 37°C, the cells were fixed with paraformaldehyde for 10 min to remove non-invaded cells and then stained with 0.1% crystal violet. The stained cells were counted in 5 randomly selected fields under a microscope.

Western blot analysis

XGC-1 cells were harvested and lysed in RIPA buffer (MT0066, Beijing Bio Lebo Technology Co., Ltd., China). Protein concentrations were determined using the BCA Protein Assay Kit (P0012S, Shanghai Biyuntian Biotechnology Co., Ltd., China). Proteins were separated by SDS-PAGE and transferred to PVDF membranes. The membranes were blocked with 5% skimmed milk for 1 h and incubated overnight at 4°C with primary antibodies against E-cadherin (1:1000, ab76055, Abcam, UK), N-cadherin (1:1000, ab280375, Abcam, UK) or GAPDH (1:1000, ab8245, Abcam, UK). After washing with TBST three times, the membranes were incubated with horseradish peroxidase-conjugated goat anti-rabbit IgG (1:2000, SE134, Beijing Soribo Technology Co., Ltd., China) at room temperature for 1 h. Finally, protein bands were visualized using the ECL chemiluminescence kit (36208ES60, Yi Sheng Biotechnology Co., Ltd., Shanghai, China).

qRT-PCR

Total RNA was extracted from tissues or cells using Trizol reagent (15596026, Thermo Scientific, USA). Complementary DNA (cDNA) was synthesized using the PrimeScript RT kit (RR037A, Beijing Zhijie Fangyuan Technology Co., Ltd., China). The expression levels of circ_0005927, miR-570-3p, or FOXO3 were quantified using a real-time quantitative fluorescence PCR kit (SR1110, Beijing Solaibo Technology Co., Ltd., China) and analyzed with a real-time quantitative PCR instrument (abi7500, Shanghai BJ Industrial Co., Ltd., China). GAPDH was used as the internal reference for circ_0005927 and FOXO3, while U6 served as the internal reference for miR-570-3p. The relative expression levels were calculated using the $2^{-\Delta\Delta CT}$ method. Primer sequences are listed in **Table 2**.

Dual luciferase reporter assay

The predicted circ_0005927 or FOXO3 mRNA 3'UTR wild-type and mutant-type specific sequence clones, which bind to miR524-5p, were inserted into the pGL3 vector to construct circ_0005927-WT/FOXO3-WT and circ_

Table 2. Primer sequences for qRT-PCR

Name	Direction	Sequences (5'-3')
circ_0005927	Forward	TCTCTCTCTAAAGAAGAGTGGGAA
	Reverse	CTGATAGCCAGCAAGCCACC
miR-570-3p	Forward	CGAAAACAGCAATTACCTTTGC
	Reverse	TGGTGTCGTGGAGTCG
FOXO3	Forward	ACTCATGCAGCGGAGCTCTAG
	Reverse	GTTCAGAGATGAAGGTCCGAACA
GAPDH	Forward	ACCACAGTC CATGCCATCAC
	Reverse	TCCACCACCCTGTTGCTGTA
U6	Forward	GCUUCGGCAGCACAUAUACUAAA
	Reverse	CGCUUCACGAAUUUGCGUGUCAU

Note: qRT-PCR: quantitative reverse transcription polymerase chain reaction.

0005927-MUT/FOXO3-MUT plasmids. MiR-570-3p mimic or miR-NC, along with the circ_0005927-WT/FOXO3-WT and circ_0005927-MUT/FOXO3-MUT plasmids were transfected into HEK-293T cells (CL0133, Hunan Fenghui Biotechnology Co., Ltd., China), using Lipofectamine 3000. The cells were collected 48 h after transfection, and the dual luciferase reporter assay system (E1910, Beijing Zhijie Fangyuan Technology Co., Ltd., China) was used for analysis.

RNase R digestion assay

Total RNA was extracted from XCG-1 cells using a Trizol reagent. The RNA samples were incubated at 37°C for 30 min, either with or without RNase R (S10068, Shanghai Yuanye Biotechnology Co., Ltd., China). The levels of circ_0005927 and GAPDH were subsequently quantified using qRT-PCR.

Nuclear and cytoplasmic separation

Subcellular fractionation was performed on XGC-1 cells using the PARISTM Kit (AM1921, Shanghai Yihui Biotechnology Co., Ltd., China). The expression of circ_0005927 in the nucleus and cytoplasm of XGC-1 was detected by qRT-PCR. U6 or GAPDH was used as the control.

Statistical analysis

SPSS 22.0 software was used for statistical analysis. The measured data were expressed as mean ± standard deviation ($\bar{x}$ ± sd), and counted data were expressed as n and analyzed by chi-square test. For normally distributed measured data, differences between two groups were assessed by the t-test, while one-way analysis of variance (ANOVA) or repeated-measures ANOVA followed by the Tukey test was used for comparisons among multiple groups. For non-normally distributed data, the Mann-Whitney U test was used for two-group comparisons. A *p*-value of <0.05 was considered significant.

Results

Expression of circ_0005927 was downregulated in GC and associated with poor prognosis

To identify circRNAs involved in GC progression, we analyzed the GEO dataset (GSE78092), which contains expression profiles from three pairs of GC tissues and three adjacent normal tissues. As shown in **Figure 1A**, a total of 115 differentially expressed circRNAs were identified in GC, with 23 upregulated and 92 downregulated (**Figure 1A**, **1B**). According to previous studies, circ_0005927, which was significantly downregulated in GC, was selected for further analysis. To validate the downregulation of circ_0005927 in GC, we performed qRT-PCR on 90 paired GC tissues and adjacent normal tissues. The results showed that the expression of circ_0005927 was significantly lower in GC tissues compared to adjacent normal tissues (P<0.05, **Figure 1C**). ROC curve analysis results showed that circ_0005927 had a strong diagnostic potential for GC, with an area under the curve (AUC) of 0.8098 (95% CI: 0.7488-0.8709, P<0.0001, **Figure 1D**). Compared to GES-1 cells, circ_0005927 expression was decreased in GC cell lines (XGC-1, NCI-N87, MCG-7901, and MGC-803) to varying extents (all P<0.05, **Figure 1E**). Given that XGC-1 cells exhibited the lowest expression of circ_0005927, they were selected for subsequent experiments. RNase R digestion assay results showed that circ_0005927 has a stable circular structure (P<0.05, **Figure 1F**). We also analyzed the relationship between clinical characteristics of GC patients and circ_0005927 expression, and found that low expression of circ_0005927 was significantly correlated with tumor differentiation (P=0.0123), lymph node metastasis (P=0.0221), and TNM stage (P=0.0019), while age, sex, and tumor size were not associated (**Table 3**). These results suggest that circ_0005927 may play a role in the pathogenesis of GC.

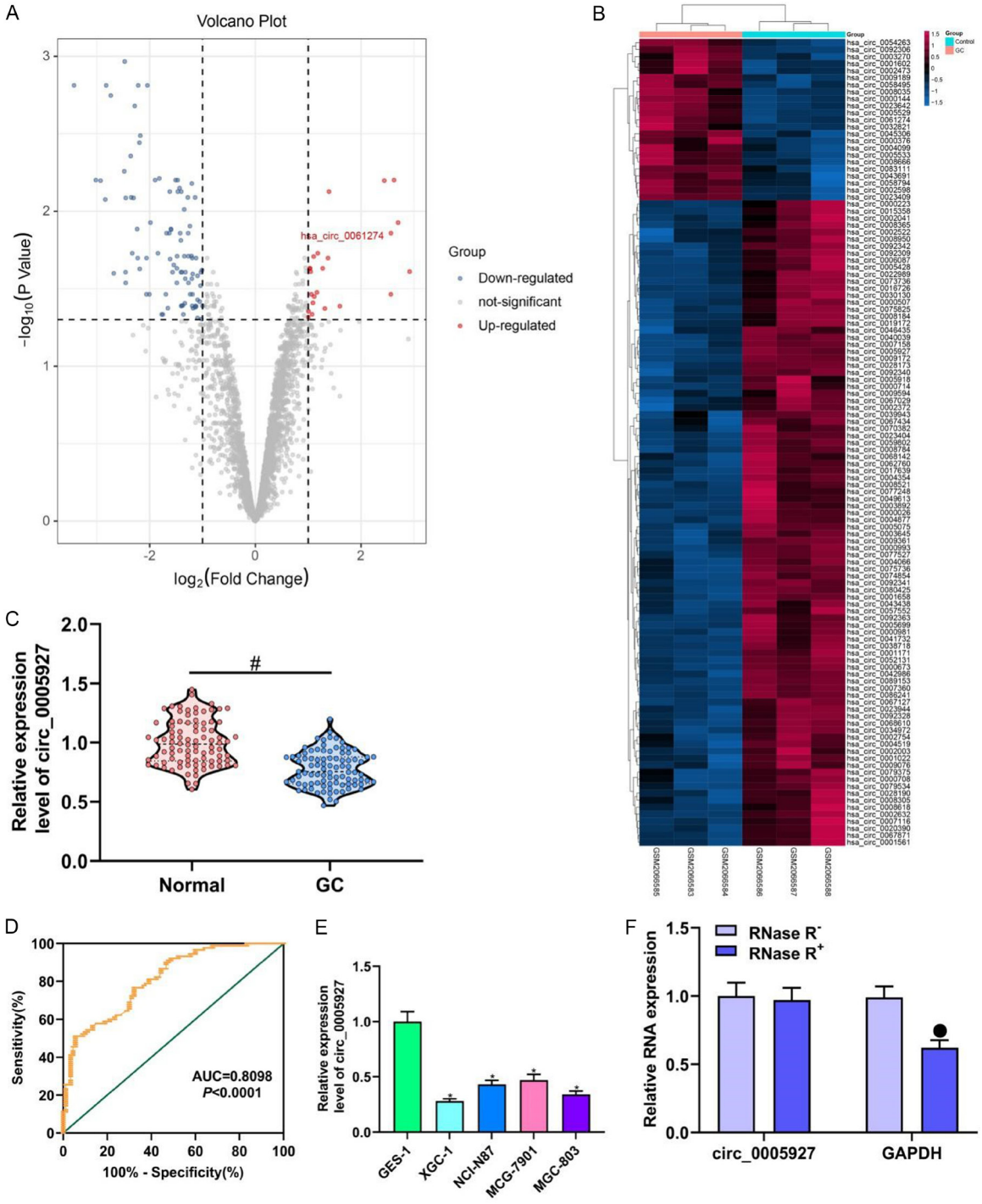

Figure 1. Downregulation of circ_0005927 in GC and its association with poor prognosis. A: Volcano plot of differentially expressed circRNAs in the GSE78092 dataset; B: Heat map of differentially expressed circRNAs in the GSE78092 dataset; C: qRT-PCR analysis of the expression of circ_0005927 in GC tissues and adjacent normal tissues (n=90); D: The diagnostic value of circ_0005927 in GC evaluated by ROC curve; E: Expression levels of circ_0005927 in the GES-1 normal cell line and GC cell lines (XGC-1, NCI-N87, MCG-7901 and MGC-803) detected by qRT-PCR; F: RNase R digestion assay. Compared with the Normal group, #P<0.05; Compared with the GES-1 cell line, *P<0.05; Compared with the RNase R- group, •P<0.05. qRT-PCR: quantitative reverse transcription polymerase chain reaction; GC: gastric cancer.

Table 3. Association between circ_0005927 expression and clinicopathologic characteristics of GC patients (n=90)

Characteristic		Cases (n=90)	circ_0005927 expression		*p*-value
			High (n=34)	Low (n=56)	
Age (years)	<60	52	19	33	0.8279
	≥60	38	15	23	
Gender	Male	58	23	35	0.6566
	Female	32	11	21	
Tumor Size (mm)	<5	33	10	23	0.3672
	≥5	57	24	33	
Differentiation	Well/moderate	23	14	9	0.0123
	Poor	67	20	47	
Lymph node metastasis	Yes	59	17	42	0.0221
	No	31	17	14	
TNM stage	I-II	27	17	10	0.0019
	III-IV	63	17	46	

Note: GC: gastric cancer.

Overexpression of circ_0005927 significantly inhibited proliferation, colony formation, invasion, and EMT of GC cells

To investigate the biological role of circ_0005927 in GC cells, we constructed a circ_0005927 overexpression vector (oe-circ_0005927). Circ_0005927 expression was significantly upregulated in the oe-circ_0005927 group compared to the oe-NC group (P<0.05, **Figure 2A**). MTT and colony formation assays showed that the upregulation of circ_0005927 in XGC-1 cells significantly inhibited cell proliferation and reduced the number of colony formations (both P<0.05, **Figure 2B-D**). Transwell assay data further showed that the upregulation of circ_0005927 significantly reduced the number of invasive XGC-1 cells (P<0.05, **Figure 2E**, **2F**). To explore the mechanism by which circ_0005927 modulates the EMT in XGC-1 cells, we assessed the expression changes of N-cadherin and E-cadherin using qRT-PCR and western blotting. The results showed that circ_0005927 upregulation significantly promoted E-cadherin expression while simultaneously downregulating both mRNA and protein levels of N-cadherin (P<0.05, **Figure 2G-I**). These findings indicate that the upregulation of circ_0005927 could effectively inhibit the malignant biological behaviors of GC cells.

miR-570-3p was the target of circ_0005927

Given the above findings, we further explored the regulatory mechanism of circ_0005927 in GC. Nuclear and cytoplasmic separation assays showed that circ_0005927 was mainly distributed in the cytoplasm of XGC-1 cells, suggesting that circVPS33B mayfunction as a competing endogenous (cerRNA) for miRNAs (P<0.05, **Figure 3A**). According to predictions from the RNA22 online tool, circ_0005927 was found to specifically bind to miR-570-3p (**Figure 3B**). Dual luciferase reporter assays revealed that in the circ_0005927-WT group, luciferase activity of miR-570-3p was significantly decreased compared to that of miR-NC (P<0.05), but the fluorescence activity of the circ_0005927-MUT group was minimally affected (P>0.05, **Figure 3C**). The expression of miR-570-3p in GC tissues and corresponding adjacent normal tissues was detected by qRT-PCR, and the results indicated a significant increase in miR-570-3p expression in GC tissues (P<0.05, **Figure 3D**), which showed a negative correlation with circ_0005927 expression (P<0.05, **Figure 3E**). ROC curve analysis results revealed an AUC of 0.8383 (95% CI: 0.7812-0.8953, P<0.0001, **Figure 3F**). Compared to GES-1 cells, miR-570-3p expression was increased to varying degrees in GC cell lines (XGC-1, NCI-N87, MCG-7901 and MGC-803) (P<0.05, **Figure 3G**). Moreover, high miR-570-3p expression was significantly

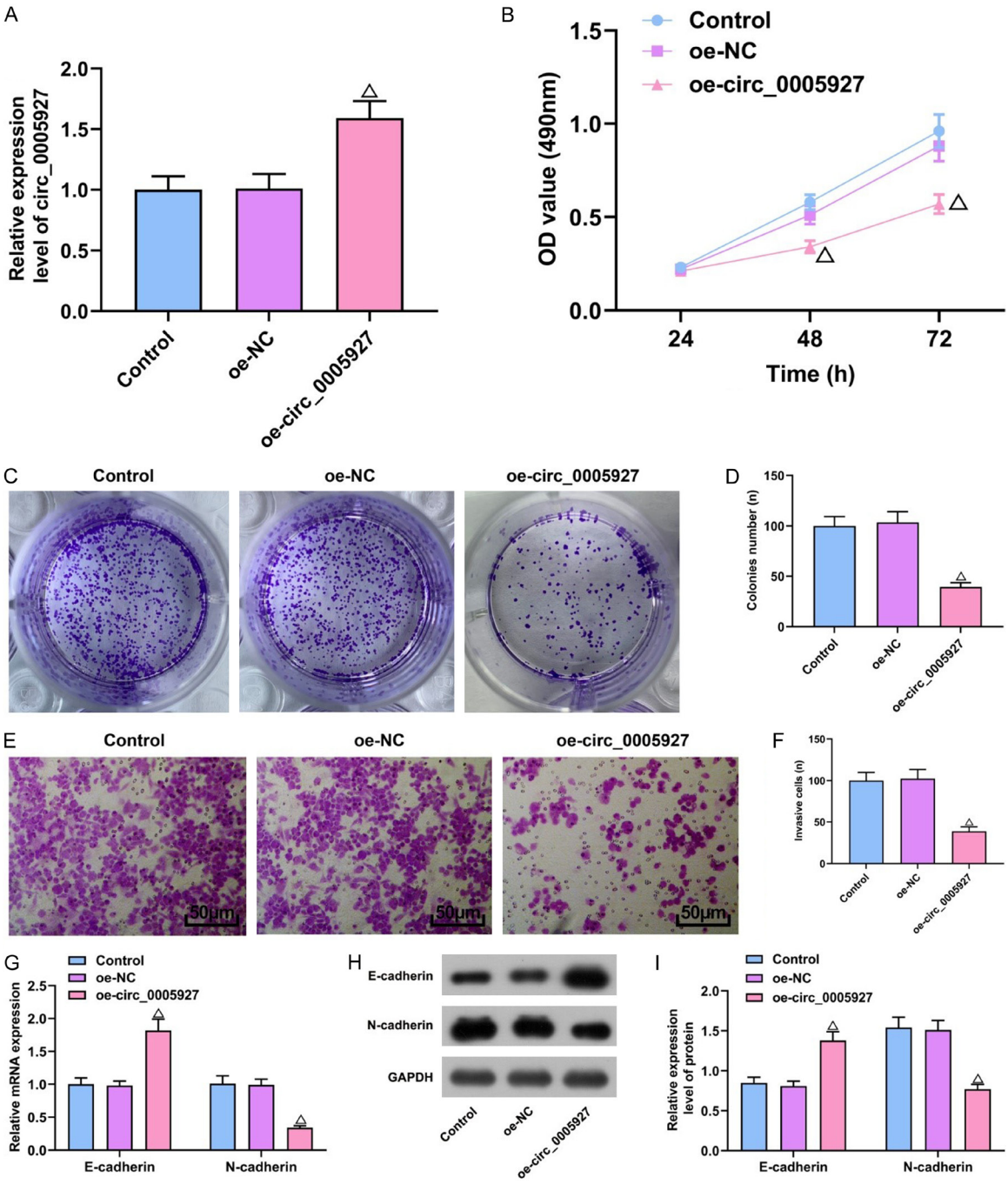

Figure 2. Overexpression of circ_0005927 significantly inhibits proliferation, colony formation, invasion and EMT in GC cells. A: Transfection efficiency of oe-circ_0005927 detected by qRT-PCR; B: MTT assay results; C, D: Colony formation assay results showing the inhibitory effect of circ_0005927 overexpression on GC cell growth; E, F: Transwell assay results (200×); G: mRNA expression levels of N-cadherin and E-cadherin detected by qRT-PCR; H, I: Protein expression levels of N-cadherin and E-cadherin were detected by western blot. Compared with the oe-NC group, $^{\Delta}P<0.05$. qRT-PCR: quantitative reverse transcription polymerase chain reaction; EMT: epithelial-mesenchymal transformation.

correlated with tumor size (P=0.0121), tumor differentiation (P=0.0205), lymph node metastasis (P=0.0192) and TNM stage (P=0.0302) in GC patients, but not with age or gender (**Table 4**). In addition, qRT-PCR analysis also unveiled that upregulation of circ_0005927 in XGC-1

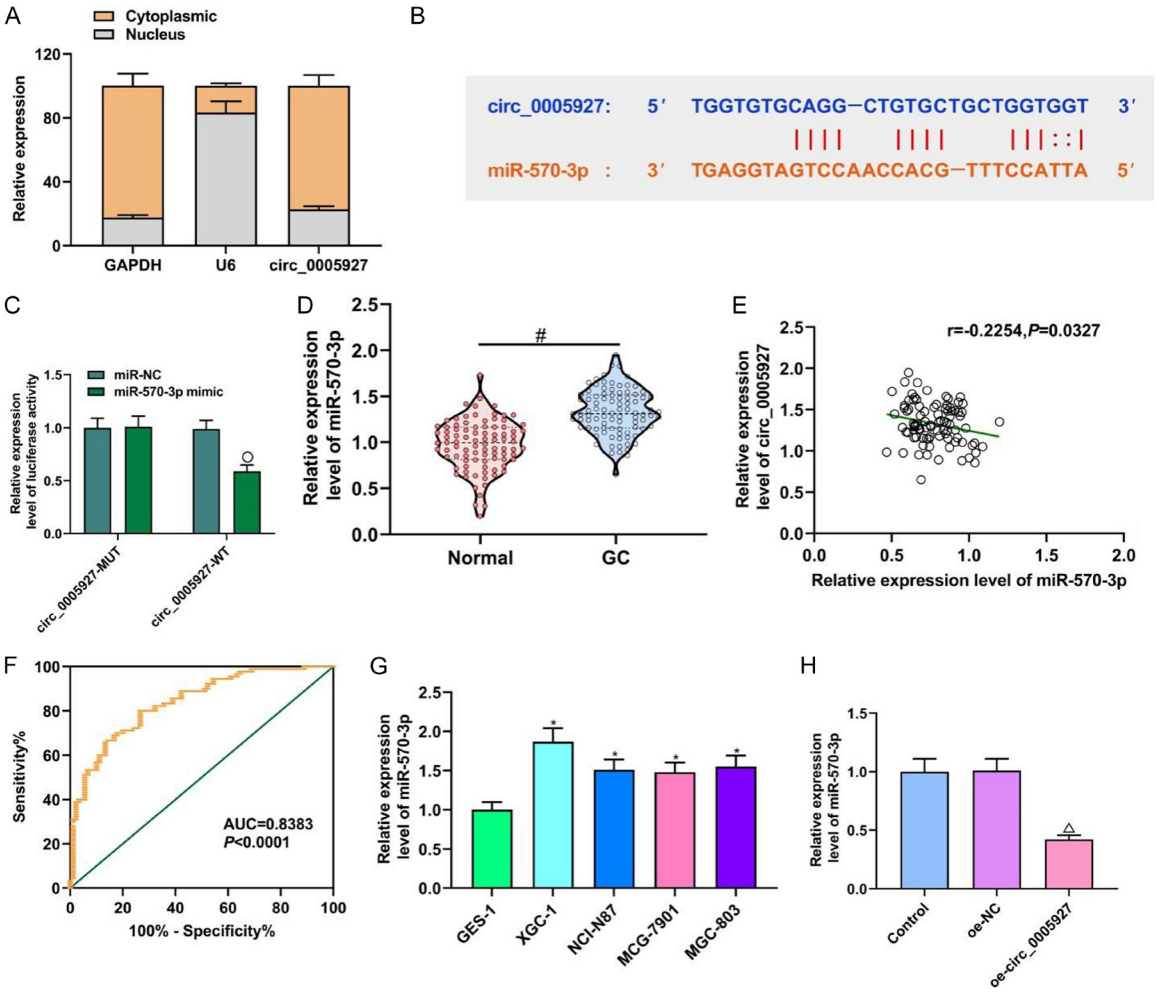

Figure 3. miR-570-3p is a target of circ_0005927. A: Results of nuclear and cytoplasmic fractionation assay; B: The specific binding sites between circ_0005927 and miR-570-3p; C: Dual luciferase reporter assay results; D: qRT-PCR analysis of miR-570-3p expression in GC tissues and adjacent normal tissues (n=90); E: Correlation analysis between the expression levels of circ_0005927 and miR-570-3p in GC tissues; F: ROC curve evaluating the diagnostic value of miR-570-3p in GC; G: qRT-PCR analysis of miR-570-3p expression in the GES-1 cell line and GC cell line (XGC-1, NCI-N87, MCG-7901 and MGC-803); H: Effect of circ_0005927 overexpression on miR-570-3p expression in XGC-1 cells. Compared with the miR-NC group, °P<0.05; Compared with the Normal group, #P<0.05; Compared with the GES-1 cell line, *P<0.05; Compared with the oe-NC group, ΔP<0.05. qRT-PCR: quantitative reverse transcription polymerase chain reaction; GC: gastric cancer.

cells significantly reduced the expression of miR-570-3p (P<0.05, **Figure 3H**).

Overexpression of miR-570-3p partially abolished the inhibitory effects of upregulated circ_0005927 on GC cells

Since circ_0005927 acts as a ceRNA for miR-570-3p in XGC-1 cells, we further investigated whether circ_0005927 regulates the malignant biological behavior of GC cells through its interaction with miR-570-3p. Transfection of miR-570-3p mimics restored miR-570-3p expression, which had been suppressed by the overexpression of circ_0005927 (P<0.05, **Figure 4A**). In addition, upregulation of miR-570-3p partially reversed the inhibitory effects of circ_0005927 overexpression on proliferation, colony formation and invasion in XGC-1 cells (all P<0.05, **Figure 4B-F**). Moreover, the upregulation of E-cadherin and downregulation of N-cadherin induced by circ_0005927 overexpression were partially reversed upon upregulation of miR-570-3p (both P<0.05, **Figure 4G-I**). These findings suggest that circ_0005927 inhibits GC cell proliferation, colony formation, and EMT by sequestering miR-570-3p.

Table 4. Association between miR-570-3p expression level and clinicopathologic characteristics of GC patients (n=90)

Characteristic		Cases (n=90)	miR-570-3p expression		*p*-value
			High (n=59)	Low (n=31)	
Age (years)	<60	52	35	17	0.8266
	≥60	38	24	14	
Gender	Male	58	40	18	0.3663
	Female	32	19	13	
Tumor Size (mm)	<5	33	16	17	0.0121
	≥5	57	43	14	
Differentiation	Well/moderate	23	10	13	0.0205
	Poor	67	49	18	
Lymph node metastasis	Yes	59	44	15	0.0192
	No	31	15	16	
TNM stage	I-II	27	13	14	0.0302
	III-IV	63	46	17	

Note: GC: gastric cancer.

circ_0005927 targeted miR-570-3p to mediate FOXO3 expression

Bioinformatic analysis using TargetScan, miRDB, and miRWalk was performed to predict the downstream targets of miR-570-3p. As shown in **Figure 5A**, a total of 328 genes were identified as potential targets of miR-570-3p. GO function enrichment analysis was subsequently conducted using the DAVID online tool, and GO terms with a P<0.05 and more than 10 enriched genes were plotted as a bar graph (**Figure 5B**). Among these, we focused on genes associated with tumor suppressor in GC, particularly the term "positive regulation of apoptosis", which included 12 significantly enriched genes. These genes were further analyzed through PPI analysis with GC-related risk genes obtained from the DisgeNet database using the STRING database (**Figure 5C**). The results highlighted FOXO3 as a gene with strong interactions. Based on previous studies, FOXO3 was selected for further analysis. The predicted complementary binding sites between miR-570-3p and FOXO3 are shown in **Figure 5D**. In addition, miR-570-3p mimic significantly inhibited the luciferase activity of FOXO3-WT, while it had minimal effect on the fluorescence activity of FOXO3-MUT (P<0.05, **Figure 5E**). qRT-PCR analysis showed that FOXO3 expression was significantly downregulated in GC tissues and cells (P<0.05, **Figure 5F**), and was positively correlated with circ_0005927 expression (P=0.0156, **Figure 5G**), while negatively correlated with miR-570-3p expression (P=0.0004, **Figure 5H**). FOXO3 expression was significantly lower in GES-1 cells compared to XGC-1, NCI-N87, MCG-7901 and MGC-803 cells (all P<0.05, **Figure 5I**). In addition, in XGC-1 cells, overexpression of circ_0005927 significantly increased the expression of FOXO3, whereas overexpression of miR-570-3p significantly decreased the expression of FOXO3 (P<0.05, **Figure 5J**).

The inhibitory effect of circ_0005927 overexpression on GC cells was partially abolished by FOXO3 knockdown

Based on the above findings, we further investigated whether circ_0005927 regulates the malignant progression of GC cells by regulating FOXO3 expression. Small interfering RNA targeting oe-circ_0005927 and FOXO3 (si-FOXO3) was co-transfected into XGC-1 cells. qRT-PCR results showed that si-Fox03 transfection significantly reduced the FOXO3 expression induced by oe-circ_0005927 (P<0.05, **Figure 6A**). Further functional assays showed that FOXO3 downregulation partially reversed the inhibitory effects of circ_0005927 overexpression on XGC-1 cell proliferation, colony formation and invasion (all P<0.05, **Figure 6B-F**). In addition, overexpression of circ_0005927 decreased N-cadherin levels and increased both the mRNA and protein levels of E-cadherin in XGC-1 cells. However, these effects were partially reversed following FOXO3 knockdown (both P<0.05, **Figure 6G-I**). These results suggest that circ_0005927 regulates GC cell prolif-

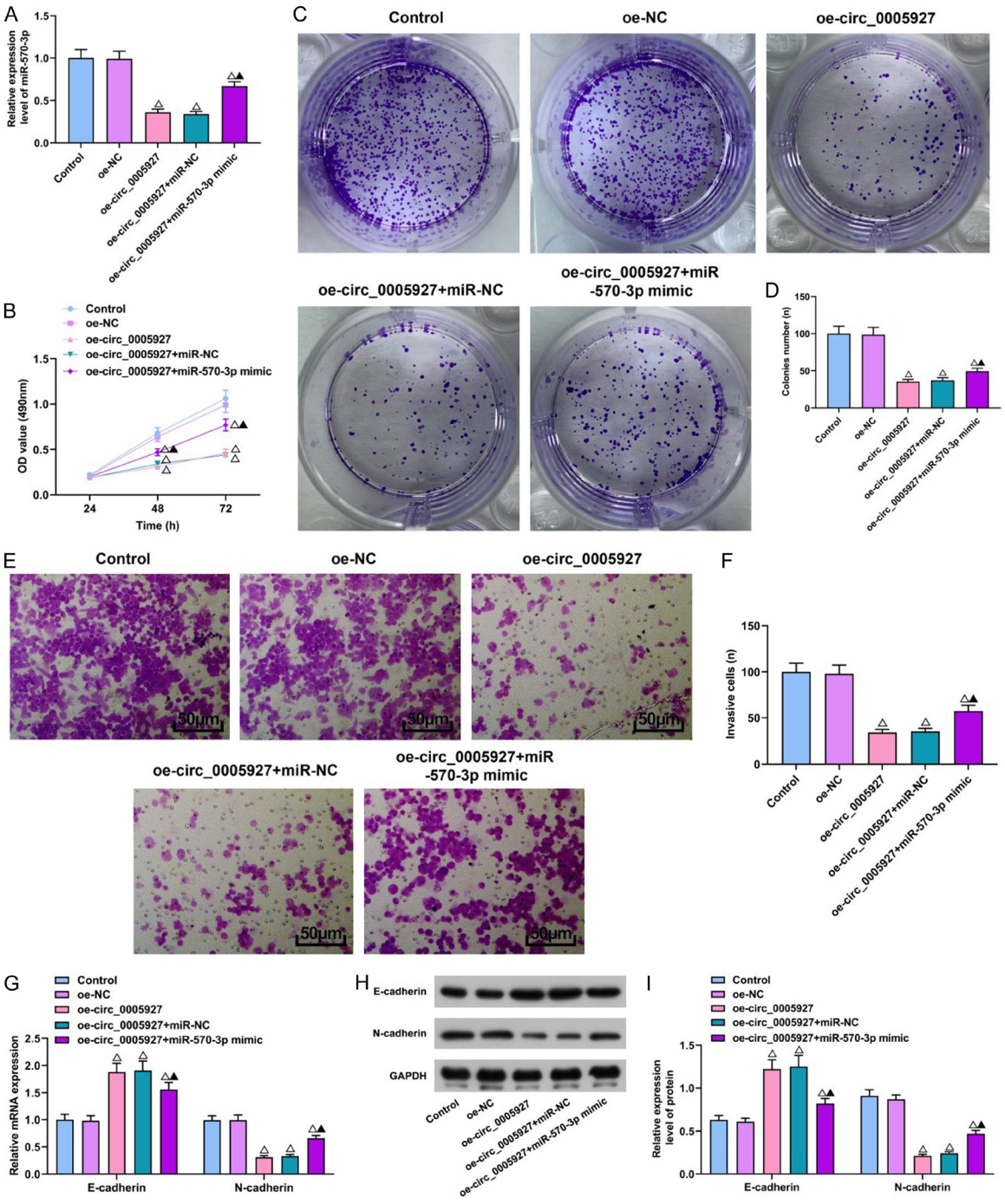

Figure 4. Overexpression of miR-570-3p partially rescues the inhibitory effect of upregulated circ_0005927 on GC cells. A: Transfection efficiency of the miR-570-3p mimic detected by qRT-PCR; B: Results of MTT assay; C, D: Results of the colony formation assay; E, F: Results of Transwell assay (200×); G: qRT-PCR analysis of N-cadherin and E-cadherin mRNA expression levels in GC cells; H, I: Western blot analysis of N-cadherin and E-cadherin protein expression levels in GC cells. Compared with the oe-NC group, $^{\Delta}P<0.05$; Compared with the oe-circ_0005927 + miR-NC group, $^{\blacktriangle}P<0.05$. qRT-PCR: quantitative reverse transcription polymerase chain reaction.

eration, colony formation, invasion and EMT by upregulating FOXO3. Therefore, circ_0005927 upregulates the expression of FOXO3 by sequestering miR-570-3p, thus inhibiting GC cell proliferation, colony formation, invasion, and EMT (**Figure 7**).

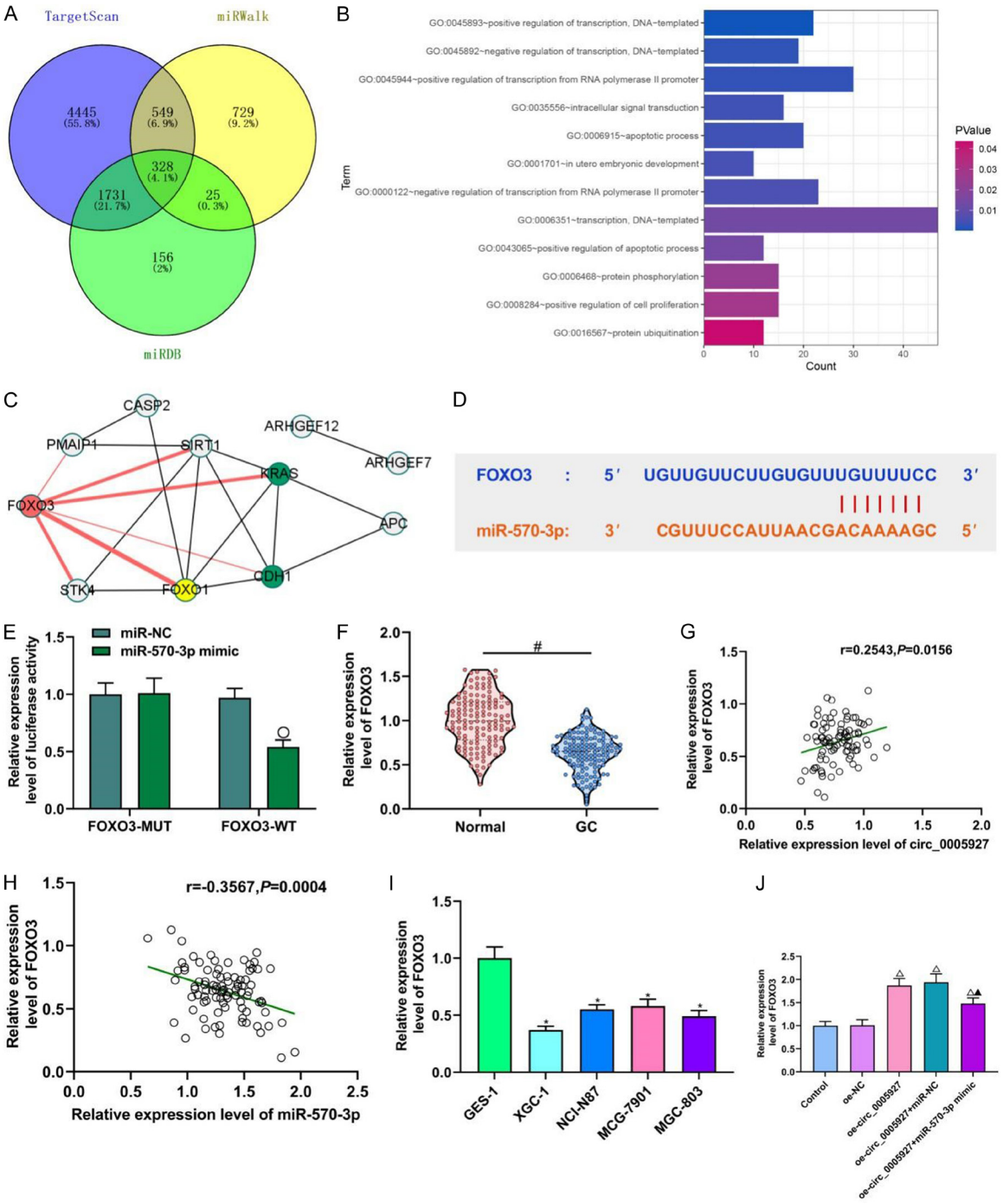

Figure 5. circ_0005927 targets miR-570-3p to mediate FOXO3 expression. A: The intersection of miR-570-3p target genes in TargetScan, miRDB, and miRWalk; B: Results of GO functional enrichment analysis; C: Protein-protein interaction (PPI) network analysis; D: Complementary binding sites between miR-570-3p and FOXO3; E: Results of dual luciferase reporter assay; F: qRT-PCR analysis of FOXO3 expression levels in GC tissues and adjacent normal tissues (n=90); G: Correlation analysis of circ_0005927 and FOXO3 expression in GC tissues; H: Correlation analysis of miR-570-3p and FOXO3 expression in GC tissues; I: qRT-PCR analysis of FOXO3 expression levels in GES-1 and GC cell lines (XGC-1, NCI-N87, MCG-7901 and MGC-803); J: The effect of circ_0005927 and miR-570-3p on FOXO3 expression in XGC-1 cells. Compared with the miR-NC group, $^{\circ}P<0.05$; Compared with the Normal group, $^{\#}P<0.05$; Compared with the GES-1 cell line, $^{*}P<0.05$; Compared with the oe-NC group, $^{\Delta}P<0.05$; Compared with the oe-circ_0005927 + miR-NC group, $^{\blacktriangle}P<0.05$. qRT-PCR: quantitative reverse transcription polymerase chain reaction; PPI: protein-protein interaction; GC: gastric cancer.

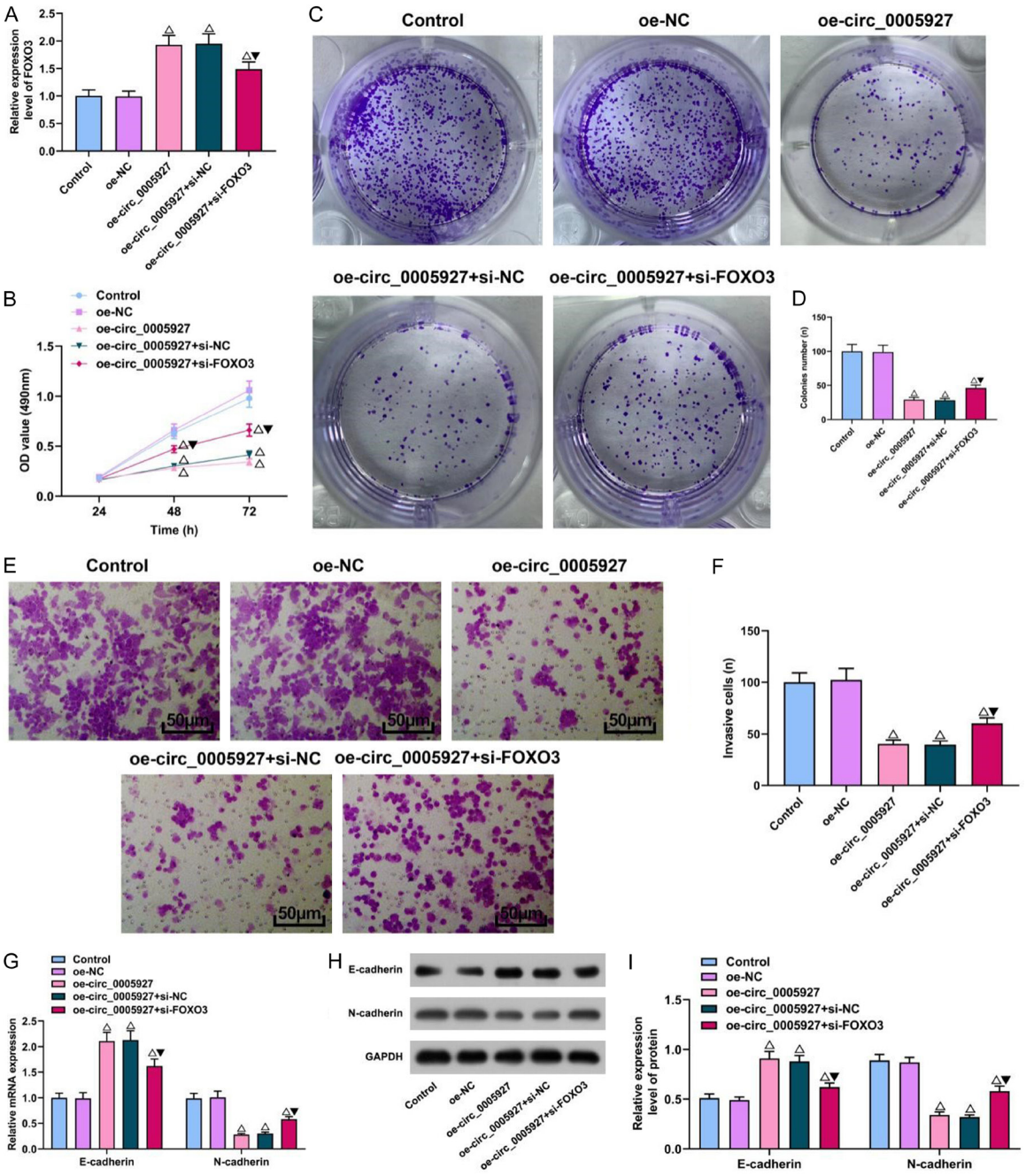

Figure 6. The inhibitory effect of circ_0005927 overexpression on GC cells was partially suppressed by FOXO3 knockdown. A: Transfection efficiency of Si-FOXO3 detected by qRT-PCR; B: Results of MTT assay; C, D: Results of colony formation assay; E, F: Results of Transwell assay (200×); G: mRNA expression levels of N-cadherin and E-cadherin detected by qRT-PCR; H, I: Protein expression levels of N-cadherin and E-cadherin detected by western blot. Compared with the oe-NC group, $^{\Delta}P<0.05$; Compared with the oe-circ_0005927 + si-NC group, $^{\blacktriangledown}P<0.05$. qRT-PCR: quantitative reverse transcription polymerase chain reaction; GC: gastric cancer.

Discussion

Improving the diagnosis and treatment of GC remains a major challenge for global health. Some studies have shown the potential of circRNAs in predicting survival and guiding therapeutic interventions for GC [9, 10]. In this study, it was found that circ_0005927 is significantly downregulated in GC and exerts inhibitory effects on GC cell proliferation, colony for-

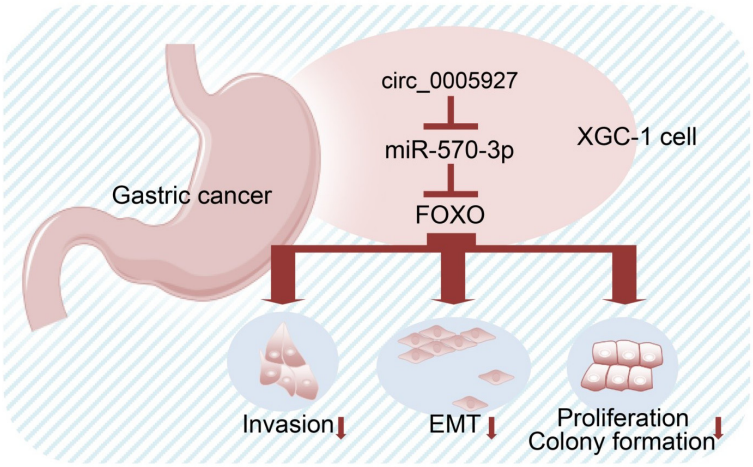

Figure 7. Mechanism of circRNA_0005927 negatively regulating miR-570-3p/FOXO3 axis to inhibit gastric cancer metastasis. EMT: epithelial-mesenchymal transformation.

mation, invasion, and EMT. In addition, circ_0005927 functions as a competitive endogenous RNA by sequestering miR-570-3p, thereby upregulating FOXO3 and inhibiting the malignant behaviors of GC cells.

Previous studies have indicated that circ_0005927 is downregulated in colorectal cancer (CRC), where it may serve as a potential diagnostic biomarker [5]. In addition, circ_0005927 inhibits CRC cell proliferation, colony formation, migration, and invasion by regulating miR-942-5p, which in turn induces BATF2 [11]. This study showed that circ_0005927 was significantly reduced in GC tissues and cells, which is consistent with previous studies [12]. Circ_0005927 has a strong diagnostic value for GC, and its low expression is significantly associated with poor prognosis in GC patients. To further investigate the role of circ_0005927 in GC, an overexpression vector of circ_0005927 was transfected into GC cells. The experimental results indicated that circ_0005927 inhibited GC cell proliferation, colony formation, and invasion. The EMT process plays a critical role in metastasis in various types of tumors, including GC [13, 14]. During EMT, the expression of cell adhesion proteins such as E-cadherin was reduced, while mesenchymal markers such as N-cadherin were greatly increased [15, 16]. In this study, qRT-PCR and western blot analyses were used to detect changes in N-cadherin and E-cadherin expression, evaluating the impact of circ_0005927 on the EMT process in GC cells. The results showed that circ_0005927 overexpression significantly increased E-cadherin levels and inhibited both the mRNA and protein expression of N-cadherin, suggesting that circ_0005927 suppresses the EMT process in GC cells.

With the help of the RNA22 online prediction tool, we identified that circ_0005927 can specifically bind to miR-570-3p. It was found that miR-570-3p plays a tumor-promoting role in ovarian cancer, breast cancer, and other malignant tumors [17, 18]. Other studies have shown that genetic polymorphisms of miR-570 may be significantly correlated with GC [19, 20]. In this study, we observed that the expression of miR-570-3p was increased in GC tissues, and its expression was negatively correlated with circ_0005927 levels. Notably, high levels of miR-570-3p were strongly associated with poor prognosis in GC patients. We also found that circ_0005927 negatively regulates miR-570-3p expression in GC cells, and that the inhibitory effects of circ_0005927 on the malignant behaviors of GC cells were partially attenuated by upregulation of miR-570-3p. These results suggest that circ_0005927 functions as a tumor suppressor in GC by inhibiting miR-570-3p. FOXO3, a member of the FOXO forkhead transcription factor subfamily, plays a crucial role in regulating a variety of cellular processes, including cell proliferation, invasion, and apoptosis [21, 22]. Reduced FOXO3 activity is commonly associated with the development of tumors [23, 24]. Previous studies have shown that miR-96-5p targets FOXO3 to promote GC cell proliferation [25], while circ_0001368 inhibits GC cell proliferation and invasion by modulating the miR-6506-5p/FOXO3 axis [26]. In our study, we found that FOXO3 expression was decreased in GC tissues and positively correlated with circ_0005927, while negatively correlated with miR-570-3p levels. Furthermore, we demonstrated that circ_0005927 can upregulate FOXO3 expression by inhibiting miR-570-3p in GC cells. Functional assays revealed that the inhibitory effects of circ_0005927 on GC cell prolifera-

tion, colony formation, invasion, and EMT were partially reversed by FOXO3 knockdown, suggesting that circ_0005927 suppresses tumor progression in GC by upregulating FOXO3.

Despite the significant findings of this study, some limitations should be addressed. First, the number of tumor samples used in our study was limited, and future research with a larger sample size is necessary to confirm these results. Second, although we have demonstrated that circ_0005927 upregulates FOXO3 by binding to miR-570-3p, the detailed molecular mechanisms underlying the circ_0005927/miR-570-3p/FOXO3 axis remain to be further investigated. Finally, our study primarily focused on *in vitro* experiments, and additional *in vivo* validation is required to corroborate our findings.

In conclusion, this study demonstrated for the first time that circ_0005927 inhibits GC cell proliferation, colony formation, invasion, and EMT by upregulating FOXO3 through the sequestration of miR-570-3p. The circ_0005927/miR-570-3p/FOXO3 axis holds significant promise as a biomarker for GC diagnosis and a therapeutic target. However, due to the limited sample size and lack of *in vivo* validation, further studies are needed to confirm these findings.

Disclosure of conflict of interest

None.

Address correspondence to: Shuguang Tan, Department of Gastrointestinal Surgery, Hengyang Central Hospital, No. 12, Yancheng Road, Yanfeng District, Hengyang 421001, Hu'nan, China. Tel: +86-0734-8275905; E-mail: 13507347332@163.com

References

[1] Lu XQ, Zhang JQ, Zhang SX, Qiao J, Qiu MT, Liu XR, Chen XX, Gao C and Zhang HH. Identification of novel hub genes associated with gastric cancer using integrated bioinformatics analysis. BMC Cancer 2021; 21: 697.

[2] Ye Z, Zeng Y, Wei S, Wang Y, Lin Z, Chen S, Wang Z, Chen S and Chen L. Short-term survival and safety of apatinib combined with oxaliplatin and S-1 in the conversion therapy of unresectable gastric cancer. BMC Cancer 2021; 21: 702.

[3] Li XW, Yang WH and Xu J. Circular RNA in gastric cancer. Chin Med J (Engl) 2020; 133: 1868-1877.

[4] Tang KW, Guo ZX, Wu ZH, Zhou C, Sun J, Wang X, Song YX and Wang ZN. Circ_0049447 acts as a tumor suppressor in gastric cancer through reducing proliferation, migration, invasion, and epithelial-mesenchymal transition. Chin Med J (Engl) 2021; 134: 1345-1355.

[5] Li J, Song Y, Wang J and Huang J. Plasma circular RNA panel acts as a novel diagnostic biomarker for colorectal cancer detection. Am J Transl Res 2020; 12: 7395-7403.

[6] Lu Y, Li L, Li L, Wu G and Liu G. Circular RNA circHECTD1 prevents Diosbulbin-B-sensitivity via miR-137/PBX3 axis in gastric cancer. Cancer Cell Int 2021; 21: 264.

[7] He Q, Yan D, Dong W, Bi J, Huang L, Yang M, Huang J, Qin H and Lin T. circRNA circFUT8 upregulates Krüpple-like factor 10 to inhibit the metastasis of bladder cancer via sponging miR-570-3p. Mol Ther Oncolytics 2020; 16: 172-187.

[8] Li M, Wang Y, Liu X, Zhang Z, Wang L and Li Y. miR-629 targets FOXO3 to promote cell apoptosis in gastric cancer. Exp Ther Med 2020; 19: 294-300.

[9] Dong Z, Liu Z, Liang M, Pan J, Lin M, Lin H, Luo Y, Zhou X and Yao W. Identification of circRNA-miRNA-mRNA networks contributes to explore underlying pathogenesis and therapy strategy of gastric cancer. J Transl Med 2021; 19: 226.

[10] Zhao G, Wu Y, Wu L, Huang J, Gan Y and Li H. Dysregulated expression levels of circular RNAs serve as prognostic and clinicopathological markers in gastric cancer: a meta-analysis. Clin Lab 2021; 67.

[11] Yu C, Li D, Yan Q, Wang Y, Yang X, Zhang S, Zhang Y and Zhang Z. Circ_0005927 inhibits the progression of colorectal cancer by regulating miR-942-5p/BATF2 axis. Cancer Manag Res 2021; 13: 2295-2306.

[12] Ding HX, Xu Q, Wang BG, Lv Z and Yuan Y. MetaDE-based analysis of circRNA expression profiles involved in gastric cancer. Dig Dis Sci 2020; 65: 2884-2895.

[13] Li F, Wang S and Niu M. Scutellarin inhibits the growth and EMT of gastric cancer cells through regulating PTEN/PI3K pathway. Biol Pharm Bull 2021; 44: 780-788.

[14] Zhou D, He Y, Li H and Huang W. Silencing of kallikrein-related peptidase 6 attenuates the proliferation, migration, and invasion of gastric cancer cells through inhibition of epithelial-mesenchymal transition. Exp Ther Med 2021; 22: 770.

[15] Chen Y and Zhang R. Long non-coding RNA AL139002.1 promotes gastric cancer development by sponging microRNA-490-3p to regulate hepatitis A virus cellular receptor 1 expression. Bioengineered 2021; 12: 1927-1938.

[16] Jin Q, Ren Q, Chang X, Yu H, Jin X, Lu X, He N and Wang G. Neuropilin-1 predicts poor prog-

nosis and promotes tumor metastasis through epithelial-mesenchymal transition in gastric cancer. J Cancer 2021; 12: 3648-3659.
[17] Wang LL, Huang WW, Huang J, Huang RF, Li NN, Hong Y, Chen ML, Wu F and Liu J. Protective effect of hsa-miR-570-3p targeting CD274 on triple negative breast cancer by blocking PI3K/AKT/mTOR signaling pathway. Kaohsiung J Med Sci 2020; 36: 581-591.
[18] Wu X, Liu D, Wang S and Liu J. Circ_0007444 inhibits the progression of ovarian cancer via mediating the miR-570-3p/PTEN axis. Onco Targets Ther 2021; 14: 97-110.
[19] Wang W, Sun J, Li F, Li R, Gu Y, Liu C, Yang P, Zhu M, Chen L, Tian W, Zhou H, Mao Y, Zhang L, Jiang J, Wu C, Hua D, Chen W, Lu B, Ju J and Zhang X. A frequent somatic mutation in CD274 3'-UTR leads to protein over-expression in gastric cancer by disrupting miR-570 binding. Hum Mutat 2012; 33: 480-484.
[20] Wang W, Li F, Mao Y, Zhou H, Sun J, Li R, Liu C, Chen W, Hua D and Zhang X. A miR-570 binding site polymorphism in the B7-H1 gene is associated with the risk of gastric adenocarcinoma. Hum Genet 2013; 132: 641-648.
[21] Tsuji T, Maeda Y, Kita K, Murakami K, Saya H, Takemura H, Inaki N, Oshima M and Oshima H. FOXO3 is a latent tumor suppressor for FOXO3-positive and cytoplasmic-type gastric cancer cells. Oncogene 2021; 40: 3072-3086.
[22] An Y, Wang B, Wang X, Dong G, Jia J and Yang Q. SIRT1 inhibits chemoresistance and cancer stemness of gastric cancer by initiating an AMPK/FOXO3 positive feedback loop. Cell Death Dis 2020; 11: 115.
[23] Pang X, Zhou Z, Yu Z, Han L, Lin Z, Ao X, Liu C, He Y, Ponnusamy M, Li P and Wang J. Foxo3a-dependent miR-633 regulates chemotherapeutic sensitivity in gastric cancer by targeting Fas-associated death domain. RNA Biol 2019; 16: 233-248.
[24] Cao Y, Li P, Wang H, Li L and Li Q. SIRT3 promotion reduces resistance to cisplatin in lung cancer by modulating the FOXO3/CDT1 axis. Cancer Med 2021; 10: 1394-1404.
[25] He X and Zou K. MiRNA-96-5p contributed to the proliferation of gastric cancer cells by targeting FOXO3. J Biochem 2020; 167: 101-108.
[26] Lu J, Zhang PY, Li P, Xie JW, Wang JB, Lin JX, Chen QY, Cao LL, Huang CM and Zheng CH. Circular RNA hsa_circ_0001368 suppresses the progression of gastric cancer by regulating miR-6506-5p/FOXO3 axis. Biochem Biophys Res Commun 2019; 512: 29-33.